Two-time scale fatigue modelling: application to damage

Anne Devulder, Denis Aubry, Guillaume Puel

Computational Mechanics manuscript No.
(will be inserted by the editor)

Two-time-scale fatigue modelling: application to damage

Anne Devulder · **Denis Aubry** · **Guillaume Puel**

Received: date / Accepted: date

Abstract A temporal multiscale modelling applied to fatigue damage evolution in cortical bone is presented. Microdamage accumulation in cortical bone, ensued from daily activities, leads to impaired mechanical properties, in particular by reducing the bone stiffness and inducing fatigue. However, bone damage is also known as a stimulus to bone remodelling, whose aim is to repair and generate new bone, adapted to its environment. This biological process by removing fatigue damage seems essential to the skeleton lifetime.
As daily activities induce high frequency cycles (about ten thousand cycles a day), identifying two-time-scale is very fruitful: a fast one connected with the high frequency cyclic loading and a slow one related to a quasi-static loading. A scaling parameter is defined between the intrinsic time (bone lifetime of several years) and the high frequency loading (few seconds). An asymptotic approach allows to decouple the two scales and to take into account history effects [1]. The method is here applied to a simple case of fatigue damage and a real cortical bone microstructure.
A significant reduction in the amount of computation time in addition to a small computational error between time homogenized and non homogenized models are obtained. This method seems thus to give new perspectives to assess fatigue damage and, with regard to bone, to give a better understanding of bone remodelling.

A. Devulder
Ecole Centrale Paris, Grande voie des vignes, 92295 Chatenay Malabry, France
Tel.: +01-41-131321
Fax: +01-41-131430
E-mail: anne.devulder@wanadoo.fr

D.Aubry
E-mail: denis.aubry@ecp.fr

Keywords Time homogenization · Damage · Fatigue · Bone

1 Introduction

Living bone supports daily cyclic loadings associated with activities like walk, jump or household occupations. Cortical bone is subsequently exposed to cyclic loadings, especially compressive stresses, which induce accumulation of damage [2][3]. Microdamage results in a reduction in strength and stiffness and can lead to bone failure incrementally through the process of fatigue [4] [5] [6].
Bone fatigue can occur at a strain magnitude which is typical of the physiological loading environment [7]. At this strain magnitude, the fatigue life of living bone is about 10^7 cycles, which corresponds to appproximatively three years of life. However, bone can adapt and repair itself through the bone remodelling process, which is essential as human skeletal elements stand throughout more than sixty years. Damage in cortical bone is known as a stimulus for bone remodelling, whose aim is to repair inadapted cortical bone by resorbing it then forming new one to prevent it from failure. The relationship between this efficient remodelling process and fatigue damage deserves further considerations. Some models have presented bone remodelling considering damage as a stimulus (Prendergast et al. [8], Doblaré et al. [9]). A damage-adaptative remodelling model where remodelling is activated when damage is above a critical level was also proposed by McMamara et al. [10]. Garcia-Aznar et al. [11] then Martinez-Reina et al. [12] presented a model dealing with time-dependent changes in bone apparent density, mineralization, fatigue damage and Young's modulus of proximal head of human femur. However, to our knowledge, fatigue damage, ensued from high and low frequencies loadings, is still not investigated. The simulation of the accumu-

lation of microdamage in bone subsequent to cyclic loading is thus interesting to understand the remodelling activation factors. In particular, the representation of the actual frequencies of *in vivo* loadings seems essential to a better understanding of the interaction between damage and remodelling. Daily activities generally induce frequencies up to three hertz. In one day, people may be submitted to approximatively 10,000 cycles. Simultaneously, bone experiences a quasi-static loading, even if some immobilization occurs, which will be defined as the "slow time" or "low frequency cycles" in the next sections. The implementation of the "fast time" attached with the high frequency cycles requests modelling as a multiscale phenomenon in time domain. The fast loading period is about several seconds whereas bone life spans years. This intrinsic time scale is thus significantly longer than the period of the high frequency cycles.
Qing and Fish [13] have decomposed initial boundary value problems with various orders of temporal scaling into a global initial boundary value problem linked to the "slow" or quasi static loading for the entire loading history and a local initial boundary value problem associated with the fast oscillatory problem for a single period. Integration of the former issue necessitates a small time step. This method has been tested on two rate-dependent material modes: the Maxwell viscoelastic and the power-law viscoplastic models. Recently, Oskay and Fish [14] have developed a multiple temporal scales model for fatigue life predictions of elastoplastic solids. Due to the discrepancy between the load period and lifetime, a mathematical homogenization technique with two temporal coordinates was carried out. The computational study was proposed in the context of continuum damage mechanics on damage growth and cracks propagation. Nonperiodic fields in time domain have arisen from irreversible inelastic deformation and have also resulted in two-time-scale problems: a slow and a fast one. Consideration of these two scales has been previously achieved by Guenounni and Aubry [1] using an asymptotic expansion method, which allows the assessment of the mean evolution together with the local cyclic loadings in the case of viscoplasticity. Yet, these models do not explore the fatigue damage issue, especially linked to a biological material as bone.
Nevertheless, in the present work, it also seems a coherent approach to split the problem into two-time-scale based on the method decribed in [1]. A "slow" time corresponding to a static cyclic loading whose period is a day long and a "fast" time which is coherent with the fast loading (frequency of 10^{-4} related to 10,000 cycles per day) are considered.

A cyclic damage model, based on a classic damage one, is developed which allows the expression of a theoretical bone lifetime. After the description of the bone damage law and the time homogenization method, a simplified case is analysed. Compressive cyclic loadings are applied to a hollowed matrix, whose material properties are identical to those of cortical bone. Finally, a real cortical bone microstructure is considered.

2 Bone damage constitutive equation

Many studies have been dedicated to bone damage [2] [3] [15] [16]. The objective here is not to provide an exhaustive analysis of the merits of each model but only to choose a representative one which will serve the purpose of illustrating the homogenization technique presented subsequently. The model is thus restricted to a simple isotropic damage law using the damage itself D as the unique internal variable.
A classical damage model requires two ingredients. The first one is related to the stress-strain relationship:

$$\sigma = E_D\,(\bar{\lambda}\,tr(\varepsilon)\,I + 2\bar{\mu}\,\varepsilon) \tag{1}$$

with σ and ε, the Cauchy stress and small strain tensors respectively. $\bar{\lambda}=\frac{\nu}{(1-2\nu)\,(1+\nu)}$ and $\bar{\mu}=\frac{1}{2\,(1+\nu)}$ are the normalized Lame coefficients and E_D the damageable Young's modulus. The normalized elasticity tensor C is then defined by:

$$C\,\varepsilon = \bar{\lambda}\,tr(\varepsilon)\,I + 2\bar{\mu}\,\varepsilon \tag{2}$$

The second one is the evolution equation of the damage which, for bone, as suggested by Frondrk [16], based on his experimental studies, is given by:

$$\frac{dD}{dt} = B\left[\frac{1-D}{\varepsilon_I}\right]\left[\frac{\sigma_I}{\sigma_r}\right]^N \tag{3}$$

with σ_I and ε_I, the major principal stress and strain respectively, σ_r a constant reference stress, B and N some material constants.

The decrease of the Young's modulus value is then represented through the equation

$$E_D = (1-D)\,E(0) \tag{4}$$

$E(0)$, the initial Young's modulus, corresponds to the elastic modulus of an ideal undamaged material (D=0) [17].

It should already be noted that, because of the assumption of the material isotropy:

$$\sigma_I = (1-D)\,(\lambda + 2\,\mu)\,\varepsilon_I \tag{5}$$

so that the previous equation (3) may be written by eliminating σ_I:

$$\frac{dD}{dt} = B\left[\frac{\lambda+2\,\mu}{\sigma_r}\right]^N (1-D)^{N+1}\,\varepsilon_I^{N-1} \tag{6}$$

or simply

$$\frac{dD}{dt} = \beta\,(1-D)^{N+1}\,\varepsilon_I^{N-1} \tag{7}$$

where $\beta = B\left[\frac{\lambda+2\mu}{\sigma_r}\right]^N$.

Other authors, like Pattin [3] and Kachanov [16], have proposed different evolution models, which could be used with the following method of time homogenization as well.

Finally, the stresses should satisfy the usual equilibrium equation (8) where *Div* is the classical divergence operator of a tensor field inside the domain Ω:

$$Div\,\sigma = 0 \tag{8}$$

Body forces are not considered here. On the boundary $\partial\Omega_\sigma$, the stress vector should match surface forces:

$$\sigma(n) = f_b \tag{9}$$

where f_b stands for the surface load and n is the outer unit vector normal to the boundary.

3 A two-time-scale fatigue simulation

The loading on the boundary is assumed to be made of two parts, depending on the spatial domain, one which varies slowly, the second rapidly:

$$f_b(t) = f_{bs}(t) + f_{bf}(\frac{t}{\xi}) \tag{10}$$

where ξ is a scaling parameter. The fast or high frequency cycles which vary very rapidly is then defined by the variable τ as:

$$\tau = \frac{t}{\xi} \tag{11}$$

As often in the case of fatigue analyses, a two-time-scale behavior is revealed. The first one is related to the daily fast cycles which is called the fast time τ, whose characteristic period is T, and the other one t is related to the static loading and low frequency cycles.
Obviously, it is not possible to compute every fast cycle for a few months. The strategy proposed here consists in building a time average technique which allows to compute low frequency cycles only, which are, however, marginally modified by the high frequency ones.

Starting with the method of Guenounni and Aubry [1], which presented a homogenization method based on a temporal asymptotic development to assess the evolution of mechanical properties of structures submitted to cyclic loadings, a new approach of temporal homogenization applied to fatigue damage is defined together with its main outline.

3.1 General assumptions

Each variable is assumed to depend simultaneously on both time scales t and τ and to be periodic with period T with respect to the fast time variable τ. The following notations are used with respect to the time derivatives of a function $\alpha(t,\tau)$, which may also be depending on the spatial domain:

$$\dot{\alpha} = \frac{\partial\alpha}{\partial t} \tag{12}$$

$$\alpha' = \frac{\partial\alpha}{\partial\tau} \tag{13}$$

Similarly, the average value $<\alpha>$ of the function α is given by:

$$<\alpha(t,\tau)> = \frac{1}{T}\int_0^T \alpha(t,\tau)d\tau \tag{14}$$

The periodicity assumption with respect to the fast period leads to:

$$<\alpha(t,\tau)'> = 0 \tag{15}$$

3.2 Series expansion with respect to the small parameter ξ

Each variable is expanded according to the following asymptotic expansion regarding ξ which gives for the strain ε:

$$\varepsilon(t,\tau) = \varepsilon_0(t,\tau) + \xi\,\varepsilon_1(t,\tau) + O(\xi^2) \tag{16}$$

with $O()$, the Landau notation.

Using the total differentiation rule $d(.)/dt$, derivatives are decomposed according to:

$$\frac{d\varepsilon}{dt} = \frac{\partial\varepsilon}{\partial t} + \frac{1}{\xi}\frac{\partial\varepsilon}{\partial\tau} = \dot{\varepsilon} + \frac{1}{\xi}\varepsilon' \tag{17}$$

Consequently, the strain derivative can be written as:

$$\frac{d\varepsilon}{dt} = \frac{1}{\xi}\varepsilon_0' + \dot{\varepsilon}_0 + \varepsilon_1' + \xi\,(\dot{\varepsilon}_1 + \varepsilon_2') + O(\xi^2) \tag{18}$$

and the damage variable:

$$\frac{dD}{dt} = \frac{1}{\xi}D_0' + \dot{D}_0 + D_1' + \xi\,(\dot{D}_1 + D_2') + O(\xi^2) \tag{19}$$

Combining the damage evolution in Eq. (7) to the expansion of the strain eigenvalue ε_I in Eq. (16):

$$\frac{1}{\xi}D_0' + \dot{D}_0 + D_1' + \xi\,\dot{D}_1 =$$
$$\beta\,(1 - D_0 - \xi\,D_1)^{N+1}\,(\varepsilon_{I_0} + \xi\,\varepsilon_{I_1})^{N-1} \tag{20}$$

As N is assumed at least larger than two, the ξ^{-1} term gives:

$$D_0' = 0 \tag{21}$$

and the ξ^0 term:

$$\dot{D}_0 + D_1' = \beta\,(1 - D_0)^{N+1}\,\varepsilon_{I_0}^{N-1} \tag{22}$$

Eq. (21) induces that:

$$D_0(t,\tau) = D_0(t) \tag{23}$$

and taking the average of the zeroth order term (Eq. (22)):

$$\dot{D}_0 = \beta\,(1 - D_0)^{N+1} <\varepsilon_{I_0}(t,\tau)^{N-1}> \tag{24}$$

Thus, the slow evolution of the damage variable depends on the fast time through the principal strain term only. The dependence with respect to the fast time τ is exhibited in the following.

3.3 Splitting of the two-time-scale

The displacement u satisfies the equilibrium equation (8) inside the domain Ω:

$$Div\left[(1-D)C\varepsilon(u(t,\tau))\right]=0 \tag{25}$$

and, on the boundary $\partial\Omega_\sigma$:

$$\left[(1-D)C\varepsilon(u(t,\tau))\right].n=f_{bs}(t)+f_{bf}(\tau) \tag{26}$$

At the zeroth order, these equations read, in Ω and $\partial\Omega_\sigma$ respectively :

$$Div\left[(1-D_0(t))C\varepsilon(u_0(t,\tau))\right]=0 \tag{27}$$

$$\left[(1-D_0(t))C\varepsilon(u_0(t,\tau))\right].n=f_{bs}(t)+f_{bf}(\tau) \tag{28}$$

Because the damage D_0 does not depend on the fast time, it is possible to split the displacement into two parts, firstly with $u_{0_s}(t)$ which satisfies a slow time equation:

$$Div\left[(1-D_0(t))C\varepsilon(u_{0_s}(t))\right]=0 \tag{29}$$

$$\left[(1-D_0(t))C\varepsilon(u_{0_s}(t))\right].n=f_{bs}(t) \tag{30}$$

and secondly with $u_{0_f}(t,\tau)$ which satisfies a coupled fast and slow time equation:

$$Div\left[(1-D_0(t))C\varepsilon(u_{0_f}(t,\tau))\right]=0 \tag{31}$$

$$\left[(1-D_0(t))C\varepsilon(u_{0_f}(t,\tau))\right].n=f_{bf}(\tau) \tag{32}$$

so that the full solution of Eq. (25) and Eq. (26) becomes:

$$u_0(t,\tau)=u_{0_s}(t)+u_{0_f}(t,\tau) \tag{33}$$

Using this decomposition, the average evolution of the damage may be written:

$$\dot{D}_0(t)=\beta\,(1-D_0(t))^{N+1}\;<\varepsilon_I(u_{0_s}(t)+u_{0_f}(t,\tau))^{N-1}> \tag{34}$$

where it is recalled that ε_I stands for the major principal strain.

It is important to stress that the fast time displacement u_{0_f} is depending linearly on the loading f_b. To go further, let us assume that the fast loading may be given as a product of a time dependent factor $\alpha_{bf}(\tau)$ with a spatial loading mode $\hat{f}_b(x)$:

$$f_{bf}(\tau,x)=\alpha_{bf}(\tau)\,\hat{f}_b(x) \tag{35}$$

Then, clearly:

$$u_{0_f}(t,\tau)=\alpha_{bf}(\tau)\,\hat{u}_{0_f}(t) \tag{36}$$

where $\hat{u}_{0_f}$ is the displacement associated with $\hat{f}_b$.

Finally, the fast part of damage evolution is simply identified by the given scalar factor $\alpha_{bf}(\tau)$:

$$\dot{D}_0(t)=\beta\,(1-D_0(t))^{N+1}\;<\varepsilon_I(u_{0_s}(t)+\alpha_{bf}(\tau)\,\hat{u}_{0_f}(t))^{N-1}> \tag{37}$$

This last formula is extremely interesting: it shows that the two displacement fields u_{0_s} and even $\hat{u}_{0_f}$ may be computed with respect to the slow time only. The slow evolution of the damage is built locally by taking the average value with respect to this known scalar coefficient α_{bf}. Obviously, the involved numerical procedure is much less costly than the one computing every fast cycle.

3.4 Fatigue criterion

It is possible to obtain a concise fatigue criterion by assuming α_{bf} small. Using a perturbation theory of eigenvalue [18], the evolution law can be approximated by:

$$\dot{D}_0=\beta\,(1-D_0)^{N+1}\;<\left[\varepsilon_I(u_{0_s})+\alpha_{bf}(\tau)\,(\varepsilon_I(\hat{u}_{0_f})(\varphi_{0_s}),\,\varphi_{0_s})\right]^{N-1}> \tag{38}$$

where, for two vectors a and b, the dot product (a,b) is defined by

$$(a,b)=\sum_{i=1,3}a_i\,b_i \tag{39}$$

φ_{0_s} stand for the principal directions of the strain tensor associated with u_{0_s}, and all the quantities except α_{bf} are depending on the slow time only. An explicit expression of the damage evolution law is here obtained with the power term approximated by the explicit formula:

$$\dot{D}_0=\beta\,(1-D_0)^{N+1}\varepsilon_I(u_{0_s})^{N-1}\left[1+(N-1)<\alpha_{bf}(\tau)>\frac{(\varepsilon_I(\hat{u}_{0_f})(\varphi_{0_s}),\,\varphi_{0_s})}{\varepsilon_I(u_{0_s})}\right] \tag{40}$$

From this expression (40), a lifetime fatigue criterion, solving for the time t_{life}, is given by:

$$1-D_0(0)=\int_0^{t_{life}}\dot{D}_0\,dt$$

where $D_0(0)$ is the initial damage value.

A first bone fatigue damage criterion is here established. It is essentially based on the zeroth order which allows a quite fast approximation of the lifetime. This lifetime results from the addition of a pure slow time contribution and a complementary term taking into account the mean effect of the fast time load combined with both the quasi-static and slow time displacement solutions.

4 First application

4.1 Definition of the problem

Three cases are investigated and compared on a linear elastic isotropic rectangular matrix with a centered elliptical hole (Fig. 1):

- The "full" computation considers the low and the high frequency cycles together in the same mechanical problem without application of the time homogenization theory. This is the case of reference.
- The "low frequency" computation only takes the low frequency cycle (t) into account. The high frequency cycles (τ) are not considered.
- The "homogenized" computation addresses the low and high frequency cycles together using the time homogenization theory presented above.

The damage evolution in the "full" and the "low frequency" computations are based on the damage equation (3) and on the equation (37) in the "homogenized" one.

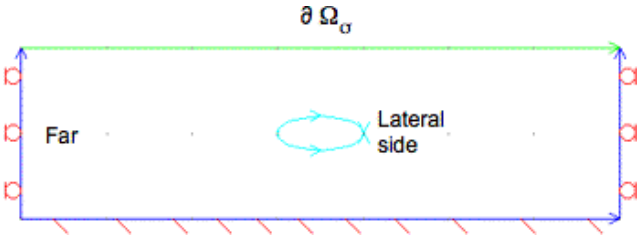

Fig. 1 Boundary conditions associated with the hollowed matrix and localization of the areas called as "far from the hole" and on its "lateral side"

In every case, the material properties of the matrix are set to an initial Young's modulus $E(0)$ equal to 20 GPa and a Poisson's ratio ν equal to 0.35. The material parameter B is set to 1, N to 4 and σ_r to 100 MPa. The matrix is initially supposed to be slightly damaged with $D(0)$ set to 10^{-4}.

A vanishing normal displacement field is prescribed on the boundaries corresponding to the lateral faces and the bottom face is totally constrained. The upper boundary $\partial\Omega_\sigma$ is submitted to a cyclic loading in compression.

The force f_{bs} related to the "low frequency" is described by:

$$f_{bs}(t) = [f_0 + f_1 sin(2\pi\omega_s t)]\ \hat{f}_b(x) \tag{41}$$

where f_0 and f_1 are some negative constants and ω_s is the slow frequency. The term $\alpha_{b_f}(\tau)$ in the expression of the force f_{bf} in Eq. (35) associated with the "high frequency" is given by:

$$\alpha_{b_f}(\tau) = f_2 sin(2\pi\omega_f \tau) \tag{42}$$

where f_2 and ω_f are a negative constant and the fast frequency respectively.

The time unit is set to the day. Computations are performed on one day, i.e. on the interval $[0;1]$. During this period, one low frequency cycle is imposed for the "low frequency" case and one low frequency cycle and ten thousand high frequency cycles occur simultaneously for the two other cases. The time steps are chosen equal to 10^{-3} for the "low frequency" and the "homogenized" computations and to 10^{-5} for the "full" one. Indeed, a smaller time step is required in the "full" case to capture the high frequency cycles. Triangular quadratic Lagrange elements are used for the usual mechanical unknowns and constant discontinuous elements for the ordinary differential equation associated with the damage variable.

4.2 Uniaxial approximation

One dimensional variables are assumed sufficient to achieve the goal of validating our time homogenization model. Instead of an equivalent stress and the whole constitutive relation tensor, the principal stress and the longitudinal value of the elastic modulus of compact bone are chosen.
The former integral Eq. (37) to be evaluated becomes consequently:

$$\int_{[0,T]} |\varepsilon_{yy}(u_s(t)) + \alpha_{bf}(\tau)\,\varepsilon_{yy}(\hat{u}_f(t))|^{N-1} d\tau \tag{43}$$

with $\varepsilon_{yy}(u_s)$ and $\varepsilon_{yy}(\hat{u}_f)$ the components in the loading direction y of the strain linked to the slow and the fast issues respectively and $|.|$ defined the absolute value.

The damage evolution is then given by:

$$\dot{D}_0(t) = \beta\,(1 - D_0(t))^{N+1} < |\varepsilon_{yy}(u_{0s}(t)) + \alpha_{bf}(\tau)\,\varepsilon_{yy}(\hat{u}_{0f}(t))|^{N-1} > \tag{44}$$

Under the non-restrictive assumption that :

$$\varepsilon_{yy}(u_{0s}(t)) + \alpha_{bf}(\tau)\,\varepsilon_{yy}(\hat{u}_{0f}(t)) < 0 \tag{45}$$

the damage law in Eq. (44) becomes:

$$\dot{D}_0 = \beta\,[1 - D_0]^{N+1} \left[-\varepsilon_{yy}(u_{0_s})^{N-1} - (N-1)\,\varepsilon_{yy}(u_{0_s})^{N-2}\,\varepsilon_{yy}(\hat{u}_{0_f}) < \alpha_{bf}(\tau) >\right] \tag{46}$$

Some positive stresses exist in the upper and the bottom boundaries of the elliptic hole, but these areas are not consider in the following.

4.3 Results

For the three cases mentioned previously, comparisons between the obtained values of the damage variable D and the strain ε_y are achieved. Two areas are analysed: far from the hole and on the lateral side of it (Fig. 1), which obviously experiences stress and strain concentrations. In the following, the graphics illustrate the homogenized output in blue, the full computation in purple and the "low frequency" model in red.

The temporal evolution of D far from the hole is given in Fig. 2, which is enlarged in the interval $[0;0.2]$ in Fig. 3 and near the lateral side in Fig. 4, enlarged in the interval $[0;0.1]$ in Fig. 5.

The "full" or reference computation and the homogenized one are quite similar. The "low frequency" case is obviously different: the comparison with the "full" computation shows why it is important to consider the high frequency cycles in the damage modelling.

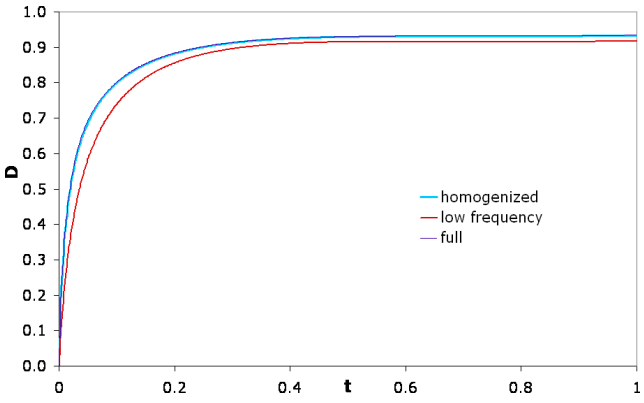

Fig. 2 Damage D evolution far from the elliptic hole

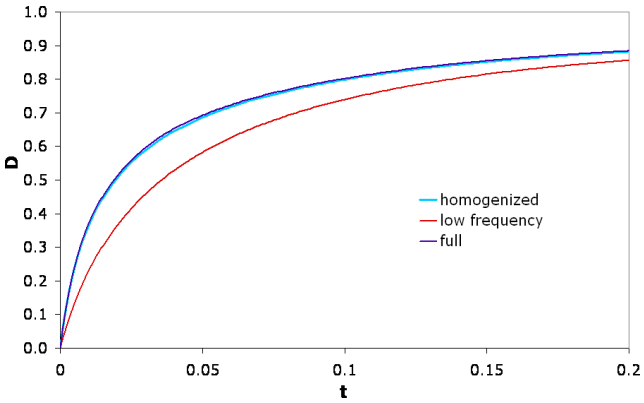

Fig. 3 Damage D evolution far from the elliptic hole (zoom)

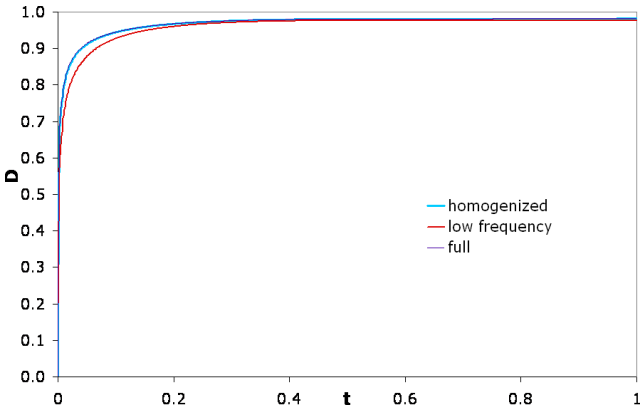

Fig. 4 Damage D evolution on the lateral side of the elliptic hole

The damage value is obviously higher near the lateral side of the hole, which experiences stress and strain concentrations, than far from it (Tables 1 and 3). The damage increases faster, especially at the beginning, when the high frequency cycles are considered, which still proves it is worth taking them into account. Nevertheless, the discrepancy decreases progressively (Tables 2 and 4).

The longitudinal normal strain evolution associated with the previous evolution of the damage variable D through the

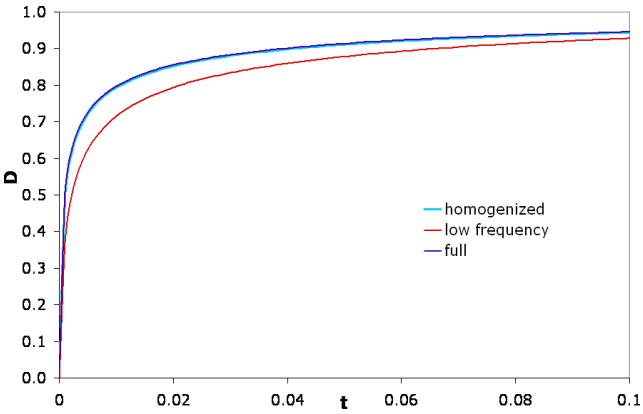

Fig. 5 Damage D evolution on the lateral side of the elliptic hole (zoom)

constitutive equation in Eq. (8) is given in Figs. 6 and 8 far from the hole and near the lateral side of the hole respectively. These figures are magnified in the interval $[0.25; 0.45]$ (Figs. 7 and 9 respectively).

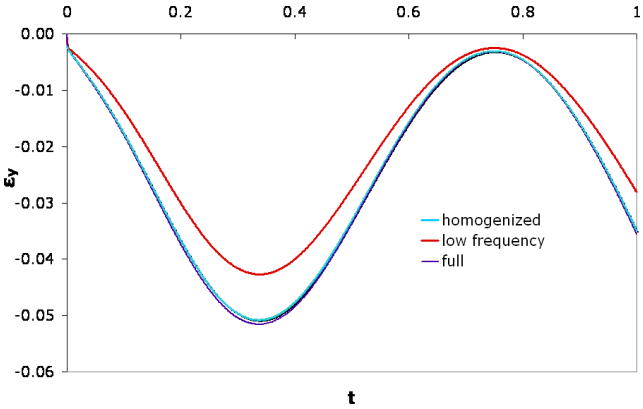

Fig. 6 Longitudinal normal strain ε_y evolution far from the elliptic hole

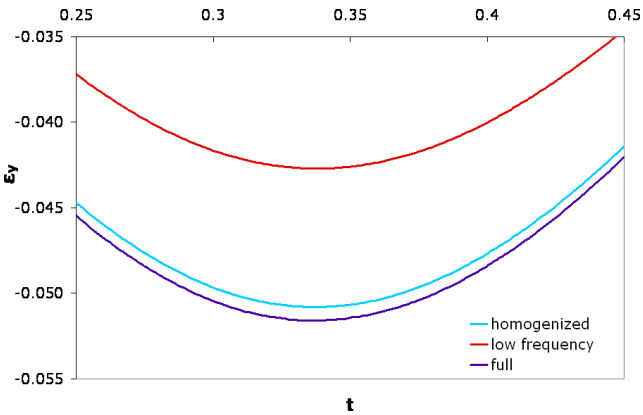

Fig. 7 Longitudinal normal strain ε_y evolution far from the elliptic hole

Table 1 Range of values for quantities associated with homogenized, full and low frequency computations (σ_y, the stress, ε_y, the strain in the loading direction and D, the damage variable), far from the hole

	homogenized	full	low frequency
σ_y (MPa)	[5 ; 105]	[5 ; 105]	[5 ; 105]
ε_y (%)	[0 ; -5.1]	[0 ; -5.2]	[0 ; -4.1]
D	0.93	0.93	0.91

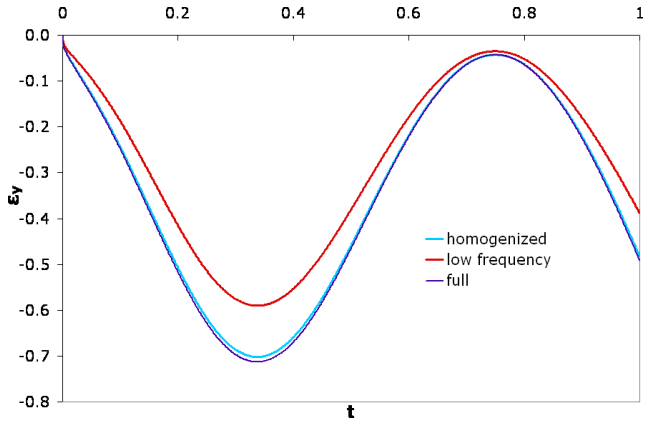

Fig. 8 Longitudinal normal strain ε_y evolution on the lateral side of the elliptic hole

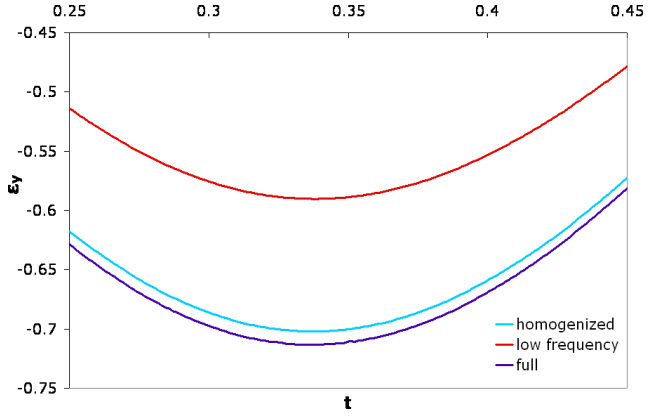

Fig. 9 Longitudinal normal strain ε_y evolution on the lateral side of the elliptic hole

As expected, the strain values are higher near the lateral side than far from it but the maximal discrepancy between the three models occurs when the load is maximal and is quite similar in both zone (Tables 2 and 4).

The mismatch for the damage variable D between the homogenized and full computations on the one hand and the low frequency calculation on the other hand is the highest at the beginning of the calculation then decreases progressively until it reaches the value 0.46% and 0.49% respectively near the lateral side of the hole and 1.75% and 1.86% far from it.

Table 2 Values of the maximal relative error (e) between quantities associated with homogenized, full and low frequency simulations, far from the hole.

ratio:	homogenized / full	full / low frequency
e_{ε_y} (%)	1.61	20
e_D (%)	0.12	1.75

Table 3 Range of values for quantities associated with homogenized, full and low frequency computations (σ_y, the stress, ε_y, the strain in the loading direction and D, the damage variable), on the lateral side of the hole

	homogenized	full	low frequency
σ_y (MPa)	[5 ; 355]	[5 ; 355]	[5 ; 355]
ε_y (%)	[0 ; -7]	[0 ; -7.1]	[0 ; -5.9]
D	0.98	0.98	0.975

Table 4 Values of the maximal relative error (e) between quantities associated with homogenized, full and low frequency simulations, on the lateral side of the hole.

ratio:	homogenized / full	full / low frequency
e_{ε_y} (%)	1.62	20
e_D (%)	0.03	0.46

Obviously, the strain field is more affected by the temporal homogenization method because it depends on the damage field through the constitutive equation. Indeed, the difference reaches about 20% between both cases, when the high frequency cycles are considered, and the case with the low frequency cycles case only (one cycle per day), is examined.

The relative error between time homogenized and non homogenized actual Young's modulus is thus very low, even negligeable (about 1%) when stress and strain are in the physiological range and low (about 6%) for very high stresses. The damage evolution law induces a very significant fast decrease of the Young's modulus. This choice allows to demonstrate the efficiency of the time homogenization achieved because when a slower evolution is considered, no difference is really observable. Moreover, the stress magnitude of the fast problem is chosen large enough to allow the examination of the influence of the stress field.

The reduction of computation costs through the temporal homogenization method is also very significant. The computation time for the time homogenized model and the low frequency one (time step of 10^{-3}) is about 360 times faster than the non homogenized (or full) model (time step of 10^{-5}).

5 Application to a real cortical bone microstructure

To illustrate the potentiality of the approach on a more realistic example, the method is here applied on a real human cortical bone microstructure. The experimentally determined microstructure is issued from the femoral diaphysis of an aged-woman. The geometrical parameters and mechanical variables result from Scanning Electron Microscopy images and compression and nanoindentation testings respectively. These data are used as initial conditions for the numerical simulation. The heterogeneous microstructure is implemented in the FE code and submitted to identical boundary conditions presented in the previous sections.
Ten thousand high frequency cycles associated with one low frequency cycle a day during thousand days are simulated. These cyclic loadings induce damage and consequently bone remodelling activation[19] [20]. Coupled with the damage evolution, a scenario of the biological process of bone remodelling is performed [21]. When the damaged bone is resorbed, new tissu is formed. The adaptation is achieved through the generation of osteons, some hollowed cylinders which give strength and stiffness to cortical bone. Comparison of the initial and the final Young's modulus, stress and strain distributions is achieved and given in Figs. 10 and 11. In the following figures, the white color corresponds to the values which exceed the maximal value of the scales. These are chosen so that the gradient of color is significant enough to depict the mechanical fields.

The scales in Figs. 10(b) and 11(b) refer to the local Young's modulus values attached to the microstructure (porosity in blue, highest value of the Young's modulus in red). The decrease of the final Young's modulus values (Fig. 11(a)) results from the damage growth (Eq. (4)). When the damage is sufficiently developed, bone remodelling is activated: three osteons are generated and appear in a kind of yellow hollowed cylinders in Fig. 11(a). An increase of the equivalent strain values relatively to the initial state (t= 1 day) due to the deterioration of the Young's modulus value is observed in Fig. 11(c). Interaction between damage and remodelling is also revealed through changes in the microstructure geometry and mechanical variables distribution (Fig. 11). Indeed, when damaged bone is resorbed, the damage growth is emphasized.
The present example, briefly outlined here, demonstrates the ability of the proposed method to evaluate the fatigue damage which could occur *in vivo* in cortical bone. The consideration of the high frequency cyclic loadings is proved to be necessary to improve the knowledge of the *in vivo* damage evolution in cortical bone associated with the bone remodelling activation.

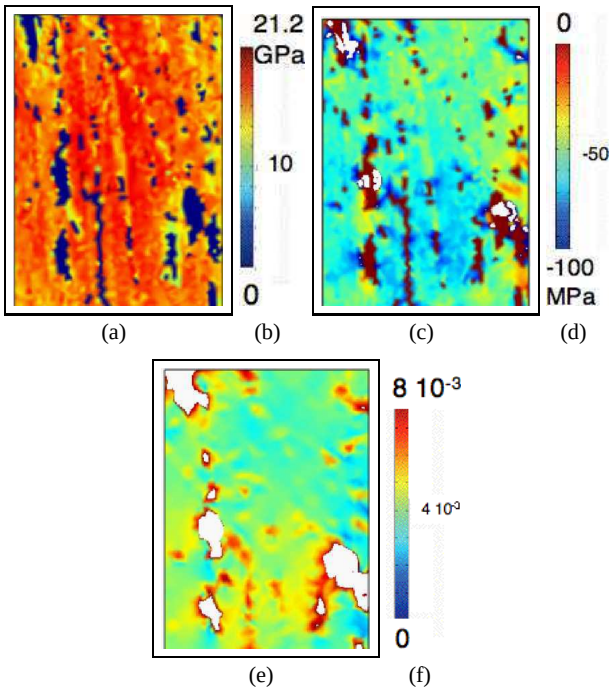

Fig. 10 Microstructure of human cortical bone before remodelling and damage (t=1 day): (a) initial Young's modulus distribution (b) scale of the Young's modulus value; (c) initial normal longitudinal stress distribution; (d) scale of the stress value; (c) initial equivalent strain distribution; (d) scale of the equivalent strain value

6 Conclusion

The time homogenization method proposed here allows the resolution of a two-time-scale issue, especially applied to damage fatigue simulation, seldom conceived by other studies. This method is based on an asymptotic expansion technique, which allows the computation of the mean evolution together with the local fast cycles loadings. The scaling parameter is defined by the ratio ξ between the material intrinsic time, associated with a quasi-static load (low frequency cycles) and the high frequency cycles of the fast loading.

The average value of the zeroth order of the variables expansion leads to the resolution of the long-term response. The oscillatory or high frequency response is obtained through the complementary terms of the asymptotic expansion. The transient evolution of the damage variable D and the strain compared between the full computation (low and high frequency cycles resolved in the same problem) and the homogenized one are very close.

A significant reduction in computation time and a very low computational error between time homogenized and non homogenized models are provided by this approach. The dependence of the slow evolution of the damage variable with respect to the fast time is simply due to the strain term and its fast evolution is only identified by a given scalar factor function of τ. Thus, the accumulation of fatigue damage,

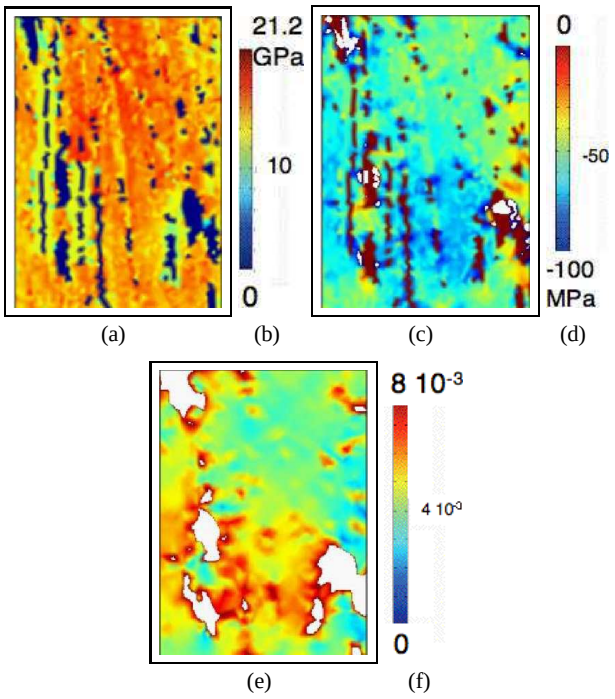

Fig. 11 Microstructure of human cortical bone after remodelling and damage (t=100 days): (a) final Young's modulus distribution (b) scale of the Young's modulus value; (c) final normal longitudinal stress distribution; (d) scale of the stress value; (c) final equivalent strain distribution; (d) scale of the equivalent strain value

issued from these high frequency cycles, can be well represented by decoupling the two scales and taking into account history effects.

The analysis of a real cortical bone microstructure will be detailled elsewhere but the relevance of the time homogenization method which allows the simulation of real daily activities and give a first approximation of the damage which could occur in bone *in vivo* is here illustrated. Furthermore, the consideration of the high frequency cyclic loadings is needed to improve the knowledge of the determining factors of the bone remodelling activation. A bone damage fatigue criterion is also obtained. This method may be consequently applied for the prediction of risks of fracture and bone ageing, which is really interesting in medical application and treatment.

Acknowledgments The authors are grateful to Thierry Hoc (Ecole Centrale Paris, France) and to the B2OA Laboratory, CNRS UMR 7052, Unviversity of Paris VII, France

References

1. Guennouni T, Aubry D (1986) Reponse homogénéisée en temps de structures sous chargements cycliques, C.R. Acad. Sc. Paris t. 303, Serie II, 20:1765-1767.
2. Burr DB, Turner CH et al (1998) Does microdamage accumulation affect the mechanical properties of bone, J Biomech 31:337-345.
3. Pattin CA, Caler WE, Carter DR (1996) Cyclic mechanical property degradation during fatigue loading of cortical bone, J Biomech 29:69-79.
4. Ballarini R, Kayacan R, Ulm F-J, Belytschko T, Heuer AH (2005) Biological structures mitigate catastrophic fracture through various strategies, Int J Fract 135:187-197
5. Suresh J. (1991) Fatigue of materials. Cambridge University Press, Cambridge
6. O'Brien FJ, Taylor D, Lee TC (2005) The effect of bone microstructure on the initiation and growth of microcracks, J Orthop Res 23(2): 475-480
7. Burr DB, Milgrom C, Fyrhie DP et al (1996) In vivo measurement of human tibial strains during vigorous activity, Bone 18:405-410.
8. Prendergast PJ, Huiskes R (1995) Mathematical modelling of microdamage in bone remodelling and adaptation, In: Odgaard A, Weinans H (Eds), Bone Structure and Remodelling, World Scientific Publishers, Singapore, pp. 213-224
9. Doblaré M, Garcia JM (2002) Anisotropic bone remodelling model based on continuum damage-repair theory, J Biomech 35(1):1-17
10. McMamara LM, Prendergast PJ (2007) Bone remodellling algorithms incorporating both strain and microdamage stimuli, J Biomech 40:1381-1391
11. Garcia-Aznar JM, Rueberg T, Doblaré M (2005) A bone remodelling model coupling microdamage growth and repair in 3D BMU activity. Biomech Model Mechanobiol 4(2-3):147-167
12. Martinez-Reina J, Garcia-Aznar JM, Dominguez J, Doblaré M (2009) A bone remodelling model including the directional activity of BMU's. Biomech Model Mechanobiol 8(2):111-127
13. Qing Y, Fish J (2002) Temporal homogenization of viscoelastic and viscoplastic solids subjected to locally periodic loading, Comput Mech 29(3):199-211
14. Oskay C, Fish J (2004) Fatigue life prediction using 2-scale temporal asymptotic homogenization, Int J Numer Methods Eng 61:329-359.
15. Frost HM (2000) Does bone design intend to minimize fatigue failures? A case for affirmative, J Bone Miner Metab 18:278- 282.
16. Davy DT, Jepsen KJ (2001) Bone damage mechanics. In: Cowin, Handbook of bone mechanics, Raton, FL: CRC Press Boca.
17. Lemaitre J (1990) A course on Damage Mechanics. 2nd ed., Springer-Verlag, Berlin
18. Kato T (1995) Perturbation Theory for Linear Operators. 2nd ed., Springer-Verlag, Berlin
19. Martin RB (2002) Is all cortical remodelling initiated by microdamage?, Bone 30(1):8-13
20. Parfitt AM (2002) Targeted and non targeted remodelling : relationship to basic multicellular unit origination and progression, Bone 30(1):5-7
21. Devulder A (2009) Approche micromécanique du remodelage osseux, PhD Thesis, Ecole Centrale Paris, France